PHYSICAL REVIEW C VOLUME 25, NUMBER 5 MAY 1982

Equilibrium shapes and fission barriers of rotating nuclei with a macroscopic two-center model

M. G. Mustafa and P. A. Baisden
Nuclear Chemistry Division, Lawrence Livermore National Laboratory, Livermore, California 94550

H. Chandra
Institut für Theoretische Physik, Universität Giessen, 63 Giessen, West Germany
(Received 23 December 1980)

Equilibrium shapes and fission barriers of rotating nuclei have been calculated using a macroscopic two-center model, with a finite-range nuclear force and a diffuse nuclear surface. Our model differs from the rotating-liquid-drop model of Cohen, Plasil, and Swiatecki in the shape parametrization and in the calculations of the surface, Coulomb, and rotational energies. We use the two-center-model shape parametrization, which allows for triaxial shape variations and a continuous transition from one-center to two-center shapes with a smooth neck. We calculate the surface energy with the Yukawa-plus-exponential folding function of Krappe, Nix, and Sierk, which incorporates the effects of the finite range of the nuclear force and the diffuse nuclear surface, and calculate both the Coulomb and rotational energies with surface diffuseness described by a Yukawa folding function. The calculation includes beta-stable nuclei up to mass number $A=250$ and selected nuclei off the line of beta stability. The results are compared with the predictions of the rotating-liquid-drop model and with experimental results statistically deduced from heavy-ion induced reactions.

[NUCLEAR REACTIONS, FISSION Calculated equilibrium shapes, fission barriers, and critical angular momenta for rotating nuclei. Macroscopic two-center model with triaxial shapes, rotating liquid-drop model, Yukawa and Yukawa-plus-exponential folding, finite range of nuclear force, surface diffuseness, heavy-ion induced fission.]

I. INTRODUCTION

Studies of the properties of nuclei at high angular momenta are of great interest. In recent years, a considerable amount of theoretical and experimental work has been carried out in this field. The present work is theoretical and deals with one aspect of high angular momentum phenomena, i.e., the equilibrium shapes and fission barriers of rotating nuclei.

The most extensively used, and perhaps the most successful theoretical model to date, is the rotating-liquid-drop model (RLDM) of Cohen, Plasil, and Swiatecki.[1] The RLDM is used routinely in the interpretation of data from many different types of heavy-ion experiments. However, questions have been raised about the general validity of RLDM.[2,3]

In this work, we present the results of the calculation of equilibrium shapes and fission barriers of rotating nuclei with an alternative and perhaps an improved macroscopic model. Unlike the RLDM, our model explicitly includes the effects of the finite range of the nuclear force and of the diffuse nuclear surface, and differs from the RLDM in the shape parametrization, and in the calculations of the surface, Coulomb, and rotational energies (see Sec. II). We use the two-center model shape parametrization, which allows for triaxial shape variations[4] and a continuous transition from one-center to two-center shapes with a smooth neck.[5] We calculate the surface energy using the Yukawa-plus-exponential folding function of Krappe, Nix, and Sierk,[6,7] which incorporates the effects of the finite range of the nuclear force and the diffuse nuclear surface. The Coulomb and rotational energies are also calculated with surface diffuseness described by a Yukawa folding function.

In the next section, we describe the model. The results are given in Sec. III with emphasis on the comparison of the predictions of our model with those of RLDM. The results are discussed in terms

of fission barriers deduced from heavy-ion-induced fission data.

II. MACROSCOPIC TWO-CENTER MODEL FOR ROTATING NUCLEI

In this section we describe the model and the procedure used in our calculation of equilibrium shapes and fission barriers for rotating nuclei. As in the RLDM, we assume that a rotating nucleus can be described by a uniformly rotating, macroscopic liquid drop. The total energy of such a rotating drop is

$$E_{\rm tot}(\alpha,J)=E_S(\alpha)+E_C(\alpha)+E_R(\alpha,J)\ , \qquad (1)$$

where E_S is the surface energy, E_C is the Coulomb energy, and E_R is the rotational energy. Alpha represents all the deformation variables necessary to describe the shape variations under rotation, and J is the angular momentum. The problem then is to calculate the quantities E_S, E_C, and E_R of Eq. (1) for all shape variables α, and find the equilibrium points of the potential energy surface for a given angular momentum J.

The main differences between this work and that of RLDM are in the nuclear shapes that we allow under rotation, and in the definitions of the surface, Coulomb, and rotational energy terms.

A. Nuclear shapes under rotation

The allowed nuclear shapes are those shown in Fig. 1. The equation governing these shapes is

$$\frac{x^2}{a^2}+\frac{y^2}{b^2}+\frac{(|z|-z_0)^2+\lambda(|z|-z_0)^4\theta(|z|-z_0)}{c^2}=1\ , \qquad (2)$$

where $\theta(\xi)$ is a step function and is defined as

$$\theta(\xi)=\begin{cases}1, & \xi<0\\ 0, & \xi>0\end{cases}$$

and $2z_0$ is the distance between centers.

Following Mosel and Schmitt[5] we have added a fourth-order term in z in Eq. (2), so that nuclear shapes are smooth at the neck. The parameter λ is therefore fixed by the condition that the shapes and their first derivatives should join smoothly at $z=0$. This yields $\lambda=-1/(2z_0^2)$. Note that when $z_0=0$ the nuclear shapes are spheres, spheroids, or ellipsoids, i.e., one-center shapes.

In this model we have four shape variables: z_0, a, b, and c. These were collectively represented by the parameter α in Eq. (1). Only three of these four variables are independent, since one variable can be eliminated by the volume conservation condition, i.e., the nuclear volume $\frac{4}{3}\pi R_0^3$ is held fixed as the nucleus deforms. The quantity R_0 is the sharp-surface radius of the spherical nucleus and is related to the nuclear-radius constant r_0 by $R_0=r_0A^{1/3}$, where A is the nuclear mass number. In our calculation, we eliminate b and treat z_0, a, and c as free variables.

The primary difference between our shapes and those of RLDM is in our explicit use of the center-separation degree of freedom z_0. Nuclear models with such a separation coordinate have been very

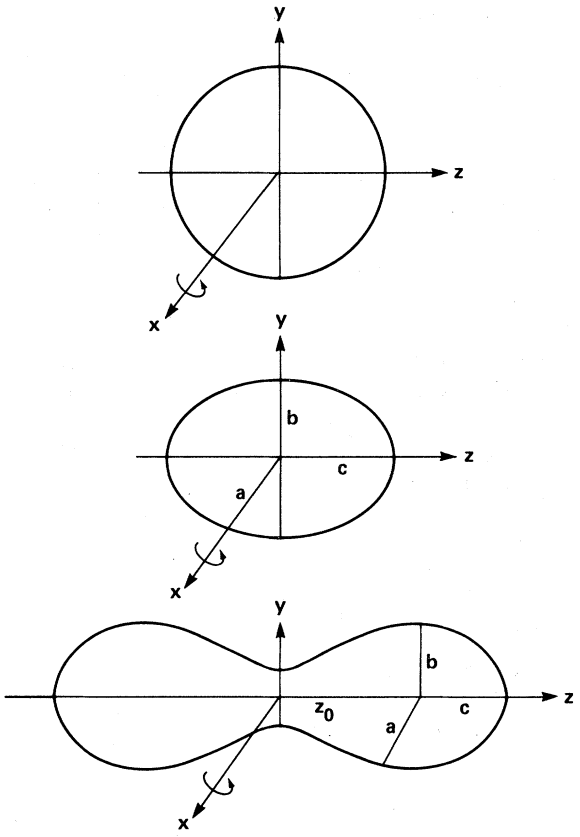

FIG. 1. Shapes of our model, as defined by Eq. (2). The x axis is the rotation axis.

successful in calculating fission properties of nonrotating systems[8] and recently in the interpretation of heavy-ion reaction data.[4]

B. Surface energy

The surface energy E_S of Eq. (1) is calculated by using the Yukawa-plus-exponential folding function, as introduced by Krappe, Nix, and Sierk.[6] Following their notation, the formal expression for the surface energy is

$$E_S=-\frac{c_s}{8\pi^2 r_0^2 a^3}\int\int\left[\frac{\sigma}{a}-2\right]\frac{e^{-\sigma/a}}{\sigma}\times d^3r\,d^3r' \tag{3}$$

with

$$\vec{\sigma}=\vec{r}-\vec{r}' .$$

The sixfold integration is over the volume of the nuclear configuration, whose magnitude is held fixed under deformation. The parameter a is the range of the folding function. The effective surface energy constant c_s is given by the usual expression[9]

$$c_s=a_s(1-\kappa_s I^2) ,$$

where $I=(N-Z)/A$, a_s is the surface energy constant, and κ_s is the surface-asymmetry constant.

For the shapes used in this model, Eq. (3) is calculated numerically. The volume integrals were first transformed into surface integrals, as in Ref. 6. The integrands were then transformed to stretched cylindrical coordinates, and then numerically integrated by means of Gauss-Legendre quadrature.

The use of the Yukawa-plus-exponential folding function has several desirable properties:

(1) It incorporates the effects of the finite range of the nuclear force and the diffuse nuclear surface.

(2) It satisfies the nuclear saturation condition for two semi-infinite slabs of nuclear matter at zero separation.

(3) It reduces the effects of sharp irregularities in the nuclear surface.

In the limit $a\to 0$, Eq. (3) will formally be the same as in RLDM. For additional discussion on the advantages and limitations of the use of the Yukawa-plus-exponential folding function, we refer to Refs. 6 and 7.

C. Coulomb energy

The Coulomb energy E_C of Eq. (1) is evaluated for a diffuse-surface charge distribution that is generated by folding a Yukawa function over a given sharp-surfaced shape and is given by[10]

$$E_C=(E_C)_{\text{sharp}}+\Delta E_C , \tag{4a}$$

where

$$(E_C)_{\text{sharp}}=\frac{{\rho_e}^2}{2}\int\int\frac{d^3r\,d^3r'}{\sigma} \tag{4b}$$

is the sharp-surface Coulomb energy and

$$\Delta E_C=-\frac{{\rho_e}^2}{2}\int\int\frac{\left[1+\frac{1}{2}\frac{\sigma}{a'}\right]}{\sigma}e^{-\sigma/a'}d^3r\,d^3r' \tag{4c}$$

is the diffuse-surface contribution to the Coulomb energy, with $\vec{\sigma}=\vec{r}-\vec{r}'$. The range a' of the Yukawa function is related to the surface width parameter b[11]

$$a'=(1/2)^{1/2}b .$$

Expressions (4b) and (4c) are evaluated numerically by the same procedure as mentioned in Sec. II B for the surface energy E_S. Note that in RLDM, the Coulomb energy is calculated for the sharp-surfaced shapes only. However, we should point out that the ΔE_C term is not that important for fission-barrier calculations. Nevertheless, inclusion of this term makes our model internally consistent, i.e., all the terms of Eq. (1) include surface diffuseness, and allows us to use a recently determined set of nuclear parameters[7] for our calculation. Furthermore, because expression (4c) is very similar to Eq. (3), the same computer code that is used to calculate the surface energy E_S is used, with minor modifications, to calculate the diffuseness contribution to the Coulomb energy, ΔE_C.

D. Rotational energy

The rotational energy E_R of Eq. (1) is given by the expression

$$E_R=\frac{J^2}{2\text{MI}} , \tag{5}$$

where MI is the moment of inertia about the axis of rotation (see Fig. 1) and J is the angular momentum. For a Yukawa folding function describing the surface diffuseness, MI can be written as[10]

$$\mathrm{MI}=(\mathrm{MI})_{\mathrm{sharp}}+4Ma'^2 \text{ , or}$$

$$=(\mathrm{MI})_{\mathrm{sharp}}+2Mb^2 ,$$

where $(\mathrm{MI})_{\mathrm{sharp}}$ is the sharp-surface moment of inertia of the shapes given by Eq. (2), M is the mass of the nucleus, a' is the range of the Yukawa folding function, and b is the surface-width parameter.

Note that the moment of inertia in RLDM is calculated for the sharp-surfaced shapes only. The addition of the diffuse-surface term, $4Ma'^2$ (or $2Mb^2$), in our calculation is shown to have significant effects at large angular momenta, particularly for light nuclei.

E. Nuclear parameters

The parameters needed to evaluate expression (1) are

(1) the nuclear-radius parameter r_0,
(2) the range of the Yukawa-plus-exponential folding function a,
(3) the range of the Yukawa folding function a' or the surface-width parameter b,
(4) the surface-energy constant a_s, and
(5) the surface-asymmetry constant κ_s.

We have taken the values of these parameters from the work of Möller and Nix, and for a complete discussion on the choices of these parameters we refer to their work.[7] The values we used are

$$r_0=1.16 \text{ fm} ,$$

$$a=0.68 \text{ fm} ,$$

$$a'=0.70 \text{ fm or } b=0.99 \text{ fm} ,$$

$$a_s=21.13 \text{ MeV} ,$$

and

$$\kappa_s=2.3 .$$

For comparison, the liquid-drop-model parameters are[9]

$$r_0=1.2249 \text{ fm} ,$$

$$a_s=17.9439 \text{ MeV} ,$$

and

$$\kappa_s=1.7826 .$$

F. Accuracy

Following Davies and Nix,[10] we have evaluated both the surface and Coulomb energies [Eqs. (3) and (4)] by transforming the volume integrals into surface integrals. The integrands were then transformed to stretched cylindrical coordinates (ρ,z,ϕ) and integrated over z and ϕ by means of an eight-point Gauss-Legendre quadrature formula in order to reach high enough numerical accuracy within reasonable computing time. Table I shows a typical example of the numerical convergence of our calculated fission barrier with respect to the integration points. The results shown are for $J=0$. Similar convergence is also found for the fission barriers with nonzero angular momentum. Note that the Coulomb and surface energies do not depend explicitly on the angular momentum and that the moment of inertia calculation for our shapes, described by Eq. (2), does not require numerical integration.

As for the shape-parameter dependence of fission barriers, we compare our value of $B_f(J=0)=30.2$ MeV for $^{153}_{65}$Tb with 29.0 MeV calculated by Nix and Sierk[12] with a different shape parametrization.[13] The experimentally-deduced value of $B_f(J=0)$ is 28.5 ± 1.7 MeV.[3] Our value then is 4% higher than that of Nix and Sierk and 6% higher than the experimental value, but at the upper end of the experimental uncertainty. Whether similar differences exist between the calculations and experiments throughout the Periodic Table will have to be investigated further.

We have found that the inclusion of the fourth-order neck-smoothing term in Eq. (2) was quite important. The effect of this term is to lower fission barriers by 1–2 MeV throughout the Periodic Table, except for very heavy nuclei. To be specific, the reduction in B_f for ^{153}Tb is 1.5 MeV for $J=0$.

TABLE I. Numerical convergence of the fission barrier $B_f(J=0)$, for $^{153}_{65}$Tb with respect to the integration points (N_z,N_ϕ) in stretched cylindrical coordinates (ρ,z,ϕ).

N_z	N_ϕ	$B_f(J=0)$ (MeV)
4	4	42.16
6	6	31.41
8	8	30.26
12	12	30.16
16	16	30.16

III. RESULTS AND DISCUSSIONS

In this section we present the results of our calculations of equilibrium shapes and fission barriers of rotating nuclei. The calculations have been done for nuclei up to mass number $A=250$ along Green's approximation to the line of beta stability[14] (the proton numbers have been rounded off to the nearest integer values) and for selected nuclei off the line of beta stability. We shall present and discuss the following results:

(1) the effects of the Yukawa-plus-exponential folding function,

(2) the effects of the diffuse-surface term of the moment of inertia,

(3) the equilibrium shapes (transitions from spherical to oblate to triaxial) and fission barriers under rotation,

(4) the critical angular momentum for which fission barrier goes to zero, and

(5) comparison of selected results with those of RLDM and recent controversial interpretations of heavy-ion induced fission data.[2,3]

In Fig. 2 we show the effects of the Yukawa-plus-exponential folding function on the calculation of fission barriers. These fission barriers are calculated for beta-stable nuclei up to mass number $A=250$ with angular momentum $J=0$. The lower line represents the results of the present model and the upper line, identified by LDM, represents the results of the liquid-drop model. The LDM calculations were done with Myers and Swiatecki parameters,[9] but with nuclear shapes defined by Eq. (2), i.e., the two-center model shapes.

The Yukawa-plus-exponential folding function results in a substantial reduction of the fission barriers for light nuclei with the magnitude of reduction increasing with decreasing mass number A. The reduction is about 4% for $A=200$, 18% for $A=150$, 25% for $A=100$, 35% for $A=50$, and 55% for $A=20$. This result is similar to that originally found by Krappe, Nix, and Sierk[6]; the actual magnitude of reduction may be slightly different.

In Fig. 3 we show a typical example of the effects of addition of the diffuse-surface term to the moment of inertia on the fission barriers. These fission barriers are shown as a function of angular momentum J for $^{97}_{45}$Rh. The solid line was calculated using the surface-width parameter $b=0.99$ fm and the dashed line using $b=0$. For comparison, we also show the results of the RLDM calculations as a

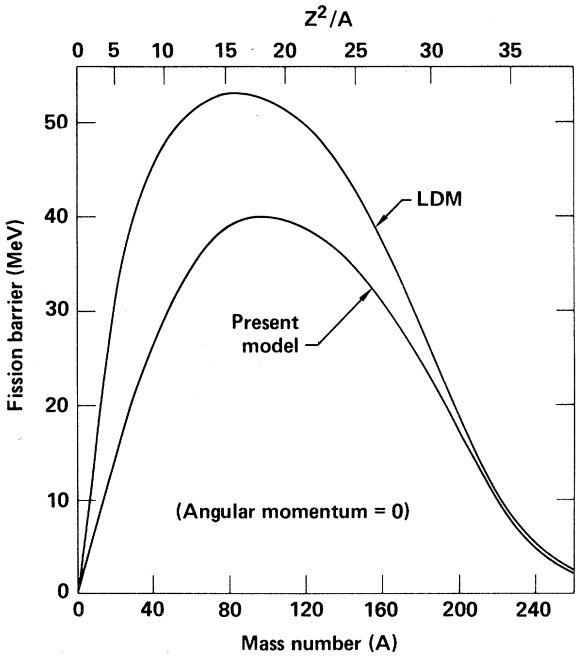

FIG. 2. Fission barriers of nonrotating nuclei along Green's approximation to the line of beta stability (Ref. 14). It shows the effects of the Yukawa-plus-exponential folding function. The lower line represents the results of the present model. The upper line, identified by LDM, represents the results of the calculations with the liquid-drop-model parameters (Ref. 9), but with shapes defined by Eq. (2).

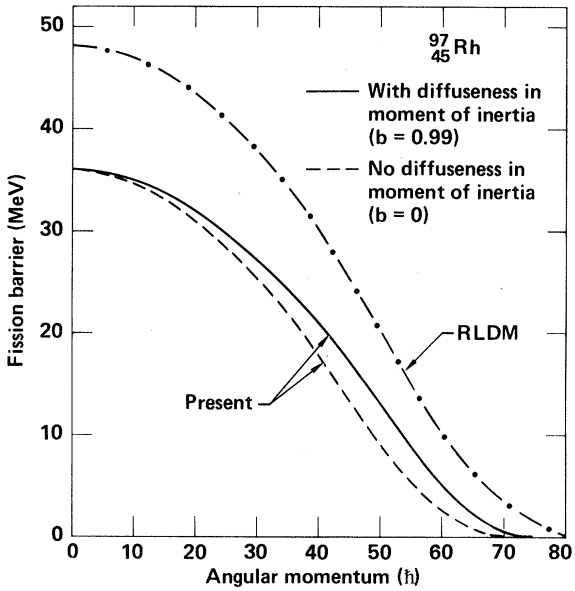

FIG. 3. Fission barriers as a function of angular momentum for $^{97}_{45}$Rh. It shows the effects of the addition of the diffuse-surface term to the sharp-surfaced moment of inertia. The quantity b is the surface-width parameter (Ref. 11). The rotating-liquid-drop-model (Ref. 1) results are given by the dotted-dashed line, identified by RLDM.

dotted-dashed line.

The results of these calculations show that the fission barriers are higher when the diffuse-surface term is present (see the two lower curves). This can be understood in terms of the relative contributions of this term to the sharp-surfaced moment of inertia at the ground state and saddle point as J increases. Note that the ground-state energy increases faster than the saddle-point energy with increasing J, as b decreases from 0.99 to 0.0 fm. This results in a higher fission barrier for a finite value of b. The difference between the two top lines represents the effects of the finite range of nuclear force and the surface diffuseness as a function of angular momentum.

The effects of the addition of the diffuse-surface term to the moment of inertia in other mass regions are shown in Table II.

In both Fig. 3 and Table II, we show that the ratio of fission barriers for $b=0.99$ fm over $b=0$, i.e., $B_f(b=0.99)/B_f(b=0)$, increases as the angular momentum J increases. The ratio can be quite large even for moderate values of J for light nuclei. For example, it is about 1.94 for $J=30\hbar$ in ^{50}V. Let us now compare this ratio among selected A for B_f ($b=0.99$ fm)$=8$ MeV, which is near the neutron binding energy. The ratio is 2.29 for ^{50}V, 1.72 for ^{97}Rh, 1.49 for ^{153}Tb, and 1.22 for ^{176}Os. The implication of these results is that the surface diffuseness in the moment of inertia may be quite important throughout the Periodic Table, particularly for light nuclei.

It is of interest to compare our model with the RLDM with respect to the critical angular momentum for the fission barrier $B_f=0$ and the angular momentum for B_f of the order of neutron binding energy, $B_f\approx 8$ MeV. These comparisons are shown in Fig. 4.

For both models ($B_f=0$ curves), we see that neither light nor heavy nuclei can support many units of angular momentum; for light nuclei it is simple because of their small size and for heavy nuclei because of their reduced stability caused by the Coulomb energy. There are, however, some differences in the models. Our model predicts lower critical angular momentum J_c for lighter nuclei ($A<140$) and for heavier nuclei ($A>210$). In the middle, we find slightly higher values for J_c. The overall difference in the predictions of the two models for J_c is at most 20%. The maximum angular momentum that a nucleus can support before fission is $(J_c)_{\max}\approx 98\hbar$ in our model, which is about the same for the RLDM. There is, however, a shift in the position of $(J_c)_{\max}$. The maximum J_c in our model is at a larger A than the RLDM.

The two lower curves in Fig. 4 show the angular momentum required to lower the fission barrier B_f of a nucleus to 8 MeV. These curves give an indication of the maximum amount of angular momentum that a compound nucleus can support and still survive fission without further deexcitation by particle emission. The maximum angular momentum in our model, $J_{\max}=75\hbar$, occurs at $A\approx 150$. The RLDM yields a $J_{\max}=77\hbar$ at $A\approx 140$. This difference in the predictions of the two models is not very large. However, the relative difference increases for

TABLE II. The effects on fission barriers, $B_f(J)$, of the addition of the diffuse-surface term to the sharp-surface moment of inertia for four nuclei: $^{50}_{23}$V, $^{97}_{45}$Rh, $^{153}_{65}$Tb, and $^{176}_{76}$Os. The surface-width parameter $b=0$ implies the absence of the diffuseness term. For comparison, $B_f(J)$ are also shown for the RLDM. The quantity J_c at the bottom of the table is the critical angular momentum for which the fission barrier goes to zero, i.e., $B_f(J_c)=0$.

	$^{50}_{23}$V			$^{97}_{45}$Rh			$^{153}_{65}$Tb			$^{176}_{76}$Os		
	Present model			Present model			Present model			Present model		
$J(\hbar)$	$b=0$	$b=0.99$	RLDM	$b=0$	$b=0.99$	RLDM	$b=0$	$b=0.99$	RLDM	$b=0$	$b=0.99$	RLDM
0	31.3	31.3	46.2	35.9	35.9	48.1	30.3	30.3	34.3	18.6	18.6	17.8
10	27.8	28.6	43.2	34.7	34.9	46.9	29.4	29.5	33.7	18.0	18.1	17.4
20	17.6	20.7	34.1	31.0	31.9	43.5	27.9	28.1	32.0	16.7	16.9	16.1
30	4.7	9.1	19.6	25.3	27.1	37.7	25.1	25.7	29.1	14.5	15.0	13.9
40	0	0.2	6.3	17.8	20.8	30.0	21.4	22.5	25.2	11.5	12.4	11.0
50		0	0.1	8.8	13.2	20.4	16.8	18.4	20.3	7.9	9.2	7.9
60			0	2.6	5.1	10.3	11.5	13.7	14.7	3.8	5.5	4.5
70				0	0.5	3.4	5.6	8.2	8.5	0.2	1.5	1.3
80					0	0.3	1.4	3.0	3.2	0	0	0
$J_c(\hbar)$	37	42	54	69	73	82	88	92	91	72	76	79

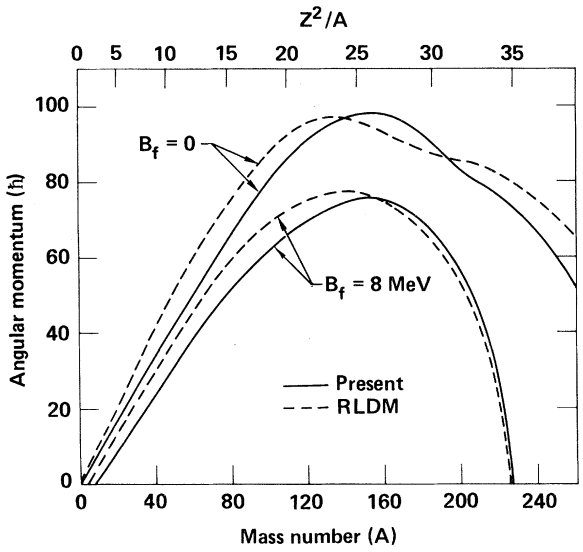

FIG. 4. The angular momentum required for the fission barrier $B_f=0$ and $B_f=8$ MeV for beta-stable nuclei (Ref. 14). The solid lines represent the present work and the dashed lines represent the results of the rotating liquid drop model (Ref. 1). The proton numbers have been rounded off to the nearest integer values.

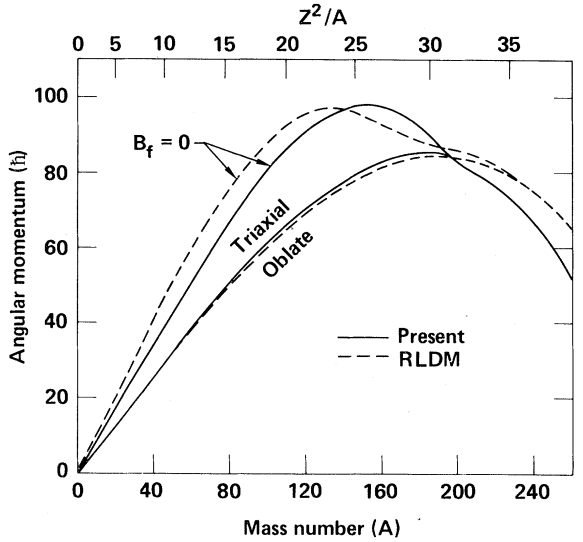

FIG. 5. The transition of equilibrium (ground-state) shapes of beta-stable nuclei (Ref. 14) from oblate to triaxial, as the angular momentum increases. The lower solid line represents the present work and the lower dashed line represents the results of the rotating-liquid-drop model (Ref. 1). The curves identified by $B_f=0$ represent the critical angular momenta for which fission barriers are zero. These curves are the same as the two top curves in Fig. 4.

TABLE III. Fission barriers (MeV) as a function of angular momentum $J(\hbar)$ for selected nuclei along Green's approximation to the line of beta stability. The critical angular momentum, $J_c(\hbar)$, for which the fission barrier of each nucleus goes to zero is given at the bottom.

	A/Z											
$J(\hbar)$	30/14	40/19	50/23	60/27	70/31	80/35	90/39	100/43	110/47	120/51	130/55	140/58
0	21.6	26.7	31.3	34.8	37.3	38.9	39.8	40.0	39.6	38.5	37.0	36.2
5	20.0	25.8	30.6	34.2	36.9	38.5	39.6	39.7	39.4	38.3	36.9	36.1
10	15.6	22.9	28.6	32.7	35.6	37.6	38.7	39.0	38.8	37.8	36.4	35.6
15	8.9	18.3	25.2	30.3	33.5	35.9	37.3	37.8	37.8	36.9	35.5	34.9
20	1.4	12.3	20.7	26.6	30.8	33.5	35.3	36.2	36.3	35.6	34.5	33.9
25	0	5.2	15.3	22.3	27.3	30.7	32.9	34.2	34.5	34.0	33.1	32.3
30		0.4	9.1	17.3	23.1	27.2	29.9	31.6	32.3	32.1	31.4	31.1
35		0	3.0	11.7	18.5	23.3	26.6	28.8	29.8	30.0	29.4	29.3
40			0.2	5.9	13.4	18.9	22.9	25.4	27.0	27.4	27.2	27.3
45			0	1.8	8.3	14.2	18.9	21.9	23.8	24.7	24.7	25.0
50				0.1	3.6	9.2	14.5	18.1	20.5	21.7	22.1	22.7
55				0	0.8	4.9	9.7	13.8	16.9	18.5	19.1	20.0
60					0	1.9	5.7	9.7	13.1	15.0	16.1	17.3
65						0.3	2.4	6.1	9.2	11.5	12.9	14.3
70						0	0.6	3.1	5.8	7.8	9.5	11.3
75							0	1.1	3.0	4.9	6.2	8.1
80								0.01	1.1	2.4	3.5	5.1
85								0	0.04	0.8	1.5	2.8
90									0	0.03	0.4	1.2
95										0	0	0.2
$J_c(\hbar)$	25	34	42	51	59	67	74	81	86	91	94	97

both small and large A. In the mass range $30<A<220$, the difference could be as much as 35%.

We now describe the changes in the equilibrium (ground-state) shapes as the angular momentum J increases. As in the RLDM, we find that starting from $J=0$, where the Coulomb plus surface energies make equilibrium shapes spherical, the equilibrium shapes become increasingly oblate for increasing J. At still higher J the preferred shapes are triaxial and then prolate shapes where finally fission barriers disappear. The two lower curves in Fig. 5 compare the transition line where the equilibrium shapes change from oblate to triaxial between our model and the RLDM. The figure also shows the critical angular momentum J_c for which the fission barrier goes to zero in the two models.

The general predictions of our model for fission barriers, $B_f(J)$, of beta-stable nuclei are given in Table III and also graphically shown in Fig. 6.

The fission barriers of ^{97}Rh, ^{153}Tb, and ^{176}Os, given in Table II, are now discussed with respect to experiments. The deexcitation products of the compound nuclei ^{97}Rh and ^{176}Os have been studied by Beckerman and Blann,[2,15] and ^{153}Tb by Plasil *et al.*[3] These authors sometimes characterize fission barriers as

$$[B_f(J)]_{\text{"correct"}}=k[B_f(J)]_{\text{RLDM}} ,$$

where the parameter k was a scaling factor. The conclusion of Beckerman and Blann is that the RLDM barriers are higher than what is deduced from the data. This statement applies to fission barriers B_f at large angular momenta, where fission barriers are in the range of 6–12 MeV and not to $B_f(J=0)$. Our model gives lower values for $B_f(J)$ for ^{97}Rh, but not for ^{176}Os. Plasil *et al.* recently deduced 0.83 for the parameter k for ^{153}Tb and quoted $B_f(J=0)=28.5\pm1.7$ MeV. Our value is 30.2 MeV (see also Table I).

We have made very selective comparison of our $B_f(J)$ with the predictions of the RLDM and experiments. In comparison with the RLDM, the predictions of our model are closer to experiments. However, a detailed comparison with experiments may not be that meaningful at this time because of the large uncertainty with which the fission barrier, $B_f(J=0)$, is deduced from the statistical-model analyses of heavy-ion-induced fission data.[15]

TABLE III. *(Continued.)*

	A/Z										
$J(\hbar)$	150/62	160/66	170/69	180/73	190/76	200/80	210/83	220/87	230/90	240/94	250/97
0	33.6	30.7	28.0	24.7	20.9	17.0	13.2	9.8	7.1	4.6	2.9
5	33.5	30.6	27.9	24.5	20.7	16.9	13.1	9.7	7.0	4.5	2.8
10	33.1	30.2	27.5	24.2	20.4	16.6	12.8	9.4	6.8	4.3	2.6
15	32.4	29.6	27.0	23.7	20.0	16.2	12.5	9.1	6.5	4.1	2.4
20	31.6	28.8	26.3	23.1	19.4	15.7	12.0	8.7	6.1	3.8	2.2
25	30.5	27.8	25.4	22.2	18.7	15.0	11.4	8.1	5.6	3.4	2.0
30	29.1	26.5	24.3	21.2	17.9	14.2	10.7	7.5	5.1	3.0	1.7
35	27.5	25.1	22.9	20.0	16.8	13.2	9.9	6.7	4.5	2.5	1.4
40	25.7	23.5	21.5	18.7	15.7	12.1	8.9	5.9	3.8	2.0	1.0
45	23.7	21.7	19.9	17.2	14.3	10.8	7.9	4.9	3.2	1.5	0.7
50	21.5	19.6	18.1	15.6	12.9	9.5	6.7	4.0	2.4	1.0	0.4
55	19.2	17.5	16.1	13.7	11.3	8.1	5.6	3.0	1.7	0.6	0.2
60	16.6	15.2	14.1	11.8	9.6	6.5	4.3	2.0	1.1	0.3	0
65	13.9	12.8	11.9	9.8	7.8	4.9	3.0	1.1	0.5	0.04	
70	11.1	10.2	9.7	7.6	6.0	3.3	1.7	0.4	0.1	0	
75	8.2	7.4	7.3	5.3	4.1	1.5	0.5	0.01	0		
80	5.3	4.7	4.6	3.1	2.1	0.08	0	0			
85	3.1	2.5	2.4	1.2	0.4	0					
90	1.3	0.9	0.8	0.06	0						
95	0.2	0.1	0.06	0							
$J_c(\hbar)$	98	97	96	92	88	82	79	76	72	66	60

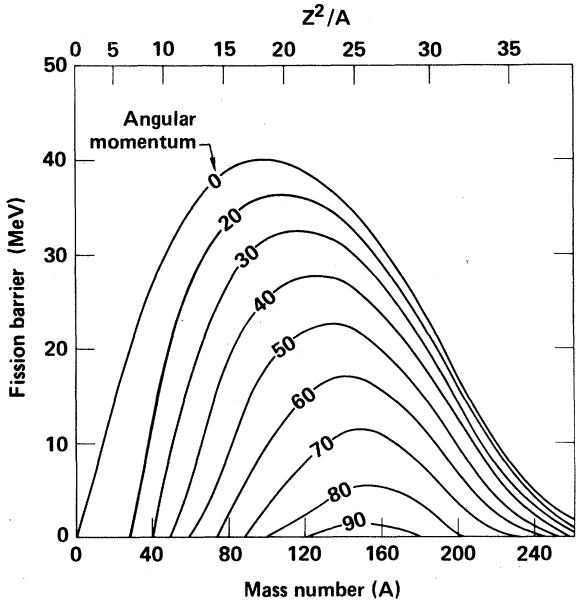

FIG. 6. Fission barriers of beta-stable nuclei (Ref. 14) for constant angular momenta from $J=0$ to $90\hbar$.

IV. CONCLUSIONS

We have presented in this paper the calculated results for equilibrium shapes and fission barriers of rotating nuclei with a macroscopic two-center model, which explicitly includes the effects of the finite-range of the nuclear force and diffuse nuclear surface. The differences between our model and the rotating-liquid-drop model of Cohen *et al.* are discussed and the predictions of the two models are compared. In general, the predictions of the two models for the fission barriers are within 30% of each other. However, at very high angular momenta and very small A the difference could be as much as a factor of 2 or more (see Fig. 1 and Table II).

We have made a selective comparison of calculated fission barriers with those deduced from heavy-ion-induced fission experiments. As was discussed, substantial differences exist not only between the predictions of theoretical models, but in the interpretations of experimental data as well. Further refinements in the calculations and careful measurements and analyses of experimental data in various mass regions are clearly needed.

As in the RLDM, we have used one set of nuclear parameters for both light and heavy nuclei and for all deformations and angular momenta. The general applicability of these nuclear parameters would require further investigations.

Many of the predictions made in this paper and in the rotating liquid drop model will be substantially altered when microscopic shell effects are included. This will be particularly true for heavier nuclei $A > 200$, where shell effects are known to be very important in reproducing measured fission barriers of nonrotating nuclei. However, for many heavy-ion induced reactions a large amount of energy is transferred to the compound nucleus, and in those cases a macroscopic description of the compound nucleus will be quite appropriate even for heavy nuclei.

ACKNOWLEDGMENTS

We acknowledge helpful discussions with U. Mosel and M. Blann. We are particularly thankful to M. Blann for the use of his computer code ALICE in calculating the fission barriers of the rotating liquid drop model, and to J. R. Nix for providing us with their $B_f(J=0)$ for ^{153}Tb. We appreciate the help of C. Castro and R. S. Newbury with the calculations. This work was performed in part under the auspices of the U. S. Department of Energy by the Lawrence Livermore National Laboratory under Contract No. W-7405-ENG-48 and under the auspices of Bundesministerim für Forschung and Technologie (BMFT) and Gesellschaft für Schwerionenforschung (GSI), West Germany.

[1]S. Cohen, F. Plasil, and W. J. Swiatecki, Ann. Phys. (N. Y.) 82, 557 (1974).

[2]M. Beckerman and M. Blann, Phys. Lett. 68B, 31 (1977); Phys. Rev. C 17, 1615 (1978).

[3]F. Plasil, R. L. Ferguson, R. L. Hahn, F. E. Obenshain, F. Pleasonton, and G. R. Young, Phys. Rev. Lett. 45, 333 (1980).

[4]H. Chandra and U. Mosel, Nucl. Phys. A298, 151 (1978).

[5]U. Mosel and H. W. Schmitt, Nucl. Phys. A165, 73 (1971).

[6]H. J. Krappe, J. R. Nix, and A. J. Sierk, Phys. Rev. C 20, 992 (1979).

[7]P. Möller and J. R. Nix, Nucl. Phys. A361, 117 (1981).

[8]M. G. Mustafa and R. L. Ferguson, Phys. Rev. C 18, 301 (1978), and references therein.

[9]W. D. Myers and W. J. Swiatecki, Ark. Fys. 36, 343 (1967).
[10]K. T. R. Davies and J. R. Nix, Phys. Rev. C 14, 1977 (1976).
[11]W. D. Myers, Nucl. Phys. A204, 465 (1973).
[12]J. R. Nix (private communication).
[13]S. Trentalange, S. E. Koonin, and A. J. Sierk, Phys. Rev. C 22, 1159 (1980).
[14]A. E. S. Green, *Nuclear Physics* (McGraw-Hill, New York, 1955), pp. 185 and 250.
[15]M. Blann and T. A. Komoto, Lawrence Livermore National Laboratory Report UCRL-87112, 1982 (unpublished).